ChemComm

COMMUNICATION

View Article Online
View Journal | View Issue

Cite this: *Chem. Commun.*, 2022, **58**, 12999

Received 25th August 2022,
Accepted 28th October 2022

DOI: 10.1039/d2cc04693h

rsc.li/chemcomm

From energy to electron transfer photocatalysis (PenT → PET): oxidative cyclobutane cleavage alters the product composition†

Jens Lefarth, *[a] Alexander Haseloer,[b] Lukas Kletsch, [b] Axel Klein, [b] Jörg Neudörfl[a] and Axel G. Griesbeck *[a]

Photocatalytic [2+2]-cycloadditions between cyclic enones and electron-rich cyclic enol ethers are initiated by triplet–triplet energy transfer from an excited iridium photocatalyst to the enone acceptor. The composition of the resulting cycloadduct mixture shows a surprising time dependency of the cyclobutane stereoisomeric ratio which indicates that the products are not photostable under the reaction conditions. The isomerisation of the cycloadducts 3 by a photoinduced redox process points to a switch from triplet energy transfer (PenT) to photoinduced electron transfer (PET) catalysis.

Photochemical [2+2]-cycloadditions can proceed by direct substrate activation through photon absorption *via* the first excited singlet or the energetically lower lying triplet state. The latter can also be generated by triplet–triplet energy transfer (PenT) using energetically adjusted sensitizers.[1–5] Alternatively to these radical-type processes, photoinduced electron transfer (PET) is possible if appropriate electron donors or acceptors are present as substrates.[6,7] Again, this PET route can be initiated by direct excitation of a substrate molecule or by use of a photoredox sensitiser. Obviously, in the photocatalysis of [2+2]-cycloadditions, PenT and PET can compete. The competition is controlled by energy arguments, *i.e.* appropriate triplet energies that allow exergonic PenT or excited state redox potentials that allow exergonic PET.

For practical reasons, photocatalytic syntheses are typically conducted until maximum conversion of the substrate that is used in lower amounts. The characteristic selectivity features such as regio- or stereoselectivity are consequently quite often determined only after complete or nearly complete conversions. These results are relevant for an overall reaction profile as well as for synthetic applications but might be misleading for a mechanistic description.

The problem that we address in this paper is the possible change in the mechanistic function of the photocatalyst that occurs after photoproduct formation using a properly designed photocatalyst (PC) for [2+2]-cycloaddition. As we have recently reported,[8] the cycloaddition between chalcone (**1**) and 2,3-dihydrofuran (2,3-DHF) (**2**) photocatalysed by $[Ir(dF(CF_3)ppy)_2(dtbbpy)]PF_6$ (abbreviated as [Ir-F], Scheme 1) results in four cyclobutane diastereomers with the compound **3a** as the major product after moderate conversions (Scheme 1). Likewise, cyclic enones and electron-rich alkenes give cycloadducts in high yields and good stereoselectivities. Redox processes that involve the enones as acceptors or the alkenes as donors are energetically improbable. On the other hand, triplet state energy comparison resulted in an exergonic energy transfer mechanism as the most likely activation meachanism. Herein, we would like to report on the unexpected isomerisation of diastereomers that was observed after prolonged irradiation of the reaction mixture.

During this study, we focussed on two potential photocatalysts (Table 1): Michler's ketone (**7**, MK)[9–11] and [Ir-F] (**8**).[12,13] In

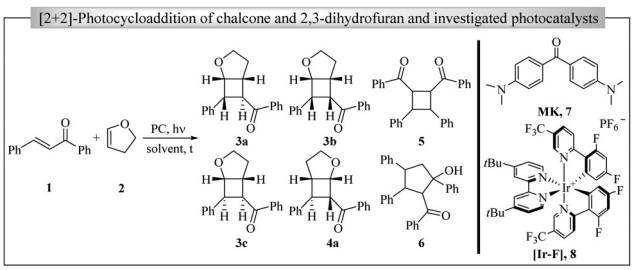

Scheme 1 Model reaction for the photosensitised [2+2]-cycloaddition of acceptor–donor systems and investigated photocatalysts.

[a] *University of Cologne, Faculty of Mathematics and Natural Sciences, Department of Chemistry, Institute for Organic Chemistry, Greinstr. 4-6, Köln D-50939, Germany. E-mail: griesbeck@uni-koeln.de; Fax: +49-221-4701166*

[b] *University of Cologne, Faculty of Mathematics and Natural Sciences, Department of Chemistry, Institute for Inorganic Chemistry, Greinstr. 4-6, Köln D-50939, Germany*

† Electronic supplementary information (ESI) available. CCDC 2192929–2192933. For ESI and crystallographic data in CIF or other electronic format see DOI: https://doi.org/10.1039/d2cc04693h

Table 1 Excited state and redox properties of the photocatalysts[a]

Catalyst	E_T [eV]	$^3\tau$ [μs]	ϕ_{ISC}	E_{ox}	E_{red}	$^3E_{ox}$	$^3E_{red}$
MK	2.73	45	0.99	0.91	−2.16	−1.82	0.57
[Ir-F]	2.58	2.3	0.68	1.69	−1.37	−0.89	1.21

[a] From ref. 7–11. Redox potentials were referenced to SCE.

the first part, the hypothesis of a time-dependent secondary PET reaction is proposed based on the experimental observations on the product selectivities of cyclobutanes **3a** and **3b** as well as dimers **5** and **6** (Scheme 1). In the second part, this theory will be underlined by cyclic voltammetry (of **3a** and **3c**) and crystal structure analysis (**3c**) as well as additional cyclobutane products (Fig. 1).[14]

During our previous study,[8] we observed that cyclopentanol dimer **6**, which was postulated to be formed by a P(C)ET mechanism,[15] seemed to be the preferred product from MK (Table 2, entry 2), whereas the cyclopentanol **6** was only a minor by-product with [Ir-F] as the photocatalyst. Based on the redox potentials shown in Table 1, this correlates to an exergonic oxidative quenching mechanism of MK by chalcone (E_{red} = −1.48 V *vs.* SCE; E_T = 2.17 eV),[16] whereas oxidative quenching for [Ir-F] was endergonic. However, further optimisation studies for the reaction with [Ir-F] as the photocatalyst revealed different product ratios after an irradiation period of 4 h (entry 5) compared to a much longer period of 24 h (entry 4). When using MK, however, a comparison of the reaction times was difficult to obtain due to a very low conversion of only 9% that was like the non-sensitised reaction after 4 h. In case of the non-sensitised reaction, no significant deviation in the product ratios was observed when irradiated for 4 h, 24 h or 48 h regardless of the excitation wavelength (350 or 455 nm). Therefore, we concluded that the different product ratios correlate to a secondary reaction from the cyclobutane products by PET similar to a photocycloreversion reaction.[17,18] Additionally, the photolysis experiments were performed in different solvents, which will only be illustrated for the case of MeCN and toluene (see Tables S1–S3, ESI,† for additional information). From non-polar solvents such as toluene, a general observation was a significantly preferred formation of the chalcone dimers, which may be attributed to an increased π-stacking interaction of the substrates and solvent molecules. In addition, an increased formation of cyclobutane **3b** was observed in case of the non-sensitised reaction (entry 6) as well as for the reaction with MK

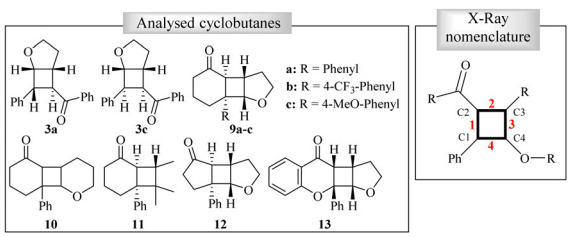

Fig. 1 Cyclobutanes analysed by cyclic voltammetry and crystal structure analysis (except **3a** and **12**).

Table 2 Irradiation time/conversion/selectivity study for the [2+2]-photocycloaddition between chalcone (**1**) and 2,3-DHF (**2**)[a]

				Product ratio[c]				
No.	PC[a]	Solvent	Yield [%][b]	**3a**	**3b**	**5**	**6**	**3a**/**3b**
1[d]	—	MeCN	51	1.0	0.34	0.11	—	2.94
2	MK	MeCN	97	1.0	0.50	0.02	1.58	2
3[e]	MK	MeCN	9	1.0	0.21	0.24	0.79	4.76
4	[Ir-F]	MeCN	>99	1.0	1.35	0.01	0.03	0.74
5[de]	[Ir-F]	MeCN	98	1.0	0.28	0.20	0.08	3.57
6	—	Toluene	83	1.0	0.89	1.63	—	1.12
7	MK	Toluene	95	1.0	15.3	—	70.8	0.07
8	[Ir-F]	Toluene	99	1.0	1.62	0.55	0.57	0.62
9[e]	[Ir-F]	Toluene	73	1.0	0.29	1.79	0.25	3.45

[a] Conditions: if not stated otherwise, irradiation for 24 h at 350 nm (for uncatalyzed and Michler's ketone [MK] reactions) or 455 nm (for [Ir-F] (1 mol%) reactions). [b] GC-MS analysis for conversion to cyclobutanes **3** and **4** and dimers **5** and **6**. [c] Ratios were referenced to the major isomer **3a** (set to 1.0). [d] Mean value of four experiments. [e] Irradiated for 4 h.

(entry 7) compared to the reaction in MeCN. The experiments with [Ir-F] as the photocatalyst, however, again showed different product ratio between cyclobutane **3a** and **3b** with varying reaction time. For these experiments, similar product ratios were obtained when compared with the results for MeCN after 4 h (entry 5 and 9) and after 24 h (entry 4 and 8).

Even though the experimental data already indicated that the observations are likely correlated to a PET process, a possible thermal instability of the photoproducts could also attribute to our findings. The reported results, however, were reproduced several times (up to ten times for some experiments), indicating that a spontaneous radical-induced reaction is improbable. In addition, the cyclobutane products in the dark showed high stability over several months with only minor degradation. Hence, a secondary photochemical reaction from the cyclobutane products appeared to be the most viable explanation for our observations.

In the next step, we wanted to study the energy profile of such a secondary PET process and determined redox potentials for **3a** and **3c** in comparison with the reported products (Fig. 1 and 2 and Fig. S1–S7, ESI†) using cyclic voltammetry.[8,19]

All oxidation and reduction processes were irreversible due to rapid follow-up reactions (see our mechanistic considerations below). Since the peak potentials of irreversible peaks are

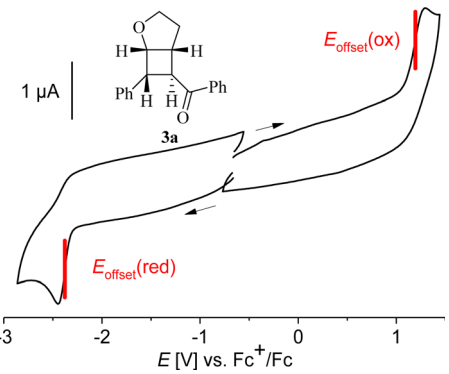

Fig. 2 Cyclic voltammograms of cyclobutane **3a** in nBu$_4$NPF$_6$/MeCN.

depending on the solvent, scan rate and concentration, we chose the same conditions for all samples and determined offset potentials as shown in Fig. 2, which approximate the half-wave potentials and give a good estimate of E^0. The CV of the cyclobutane **3a** (Fig. 2) showed an unexpectedly low oxidation potential E_{offset}(ox) of 1.2 V *vs.* ferrocene/ferrocenium (Table 3) alongside with **9c** and **13**. Product **3c** lies slightly higher with 1.43 V, which is in the range of cyclobutanes **9a**, **10**, **11**, and **12**. Taken together with the reduction potentials, the electrochemical gap of **3a** and **3c** is about 3.6 eV. Again, the cyclobutane **13** shows a similar value, while **9a**, **10**, **11**, and **12** show gap energies of more than 4.5 eV. As can be expected from the electron-donating MeO substituent in **9c** and the electron-demanding CF_3 group in **9b**, the oxidation potential increases massively along the the series **9c** < **9a** < **9b**.

Although an estimation of the Gibbs energy[20] for **3a** for a PET appeared to be slightly endergonic with [Ir-F] (^{1}[Ir-F]: ΔG_{PET} ~7 kcal mol^{-1} using the redox potentials for the singlet excited Ir-F and **3a**, normalized to the standard calomel electrode and $E_{coulombic}$ = 0), a PET reaction is still possible. For instance, substrate activation by components of the reaction mixture or slightly increased temperatures from photolysis (~30 °C) could lower the activation energy. Moreover, a significant difference between the oxidation potentials of cyclobutanes **3a** and **3c** (~0.3 V) was observed that might explain the sole conversion of cyclobutane **3a** after prolonged irradiation in the presence of [Ir-F]. Spectroelectrochemical measurements on the oxidation reaction were performed for cyclobutane **3a** and **3c** (Fig. 3).

In both cases, a new absorption maximum appeared on electro-chemical oxidation at λ_{max} = 400 nm and around λ_{max} = 305 nm that indicate the formation of a product with an extended π-system. Unfortunately, both processes turned out to be irreversible, since on return-scan we did not observe the starting materials. In the next step, we wanted to gain insight into if the oxidation event is followed by C–C bond cleavage. For this, we compared the C–C bond lengths of the studied cyclobutane **3c** from a crystal structure determination with those of further cyclobutane products (Fig. 1).

Table 3 Redox potentials of cyclobutanes[a]

	E_{pa}(ox)	E_{offset}(ox)	E_{pc}(red)	E_{offset}(red)	ΔE
3a	1.29	1.20	−2.45	−2.38	3.58
3c	1.57	1.43	−2.43	−2.34	3.77
9a	1.63	1.46	—[b]	−3.15	4.58
9b	—[b]	>1.55[b]	—[b]	<−2.97[b]	4.52
9c	1.08	1.03	—[b]	<−3.12[b]	4.15
10	1.75	1.65	—[b]	<−3.29[b]	4.94
11	1.83	1.56	—[b]	<−3.24[b]	4.80
12	—[b]	1.53	—[b]	<−3.17[b]	4.70
13	1.19	1.10	−2.31	−2.24	3.43

[a] Measured in 0.1 M nBu$_4$NPF$_6$/MeCN at 298 K, 100 mV s^{-1} scan rate at a conc. of 7 mM. Anodic peak potential E_{pa} for irreversible oxidations, cathodic peak potentials E_{pc} for irreversible reductions, measured with an accuracy of ±0.005 V and offset potentials E_{offset} (as defined in Fig. 2) in V *vs.* ferrocene/ferrocenium. ΔE = electrochemical gap between HOMO and LUMO. [b] No defined peaks observed, maximum E_{offset} potentials estimated (see ESI).

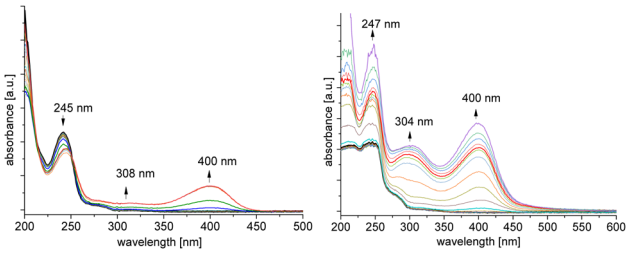

Fig. 3 UV-vis absorption spectra during electrochemical oxidation of cyclobutane **3a** (left) and **3c** (right) in nBu$_4$NPF$_6$/MeCN.

We hypothesised that the oxidation weakened the σ-bond of the cyclobutane moiety (bond 1 or bond 4, numbering see Fig. 1), resulting in the more stable radical cation intermediate. For comparison, the unsubstituted cyclobutane has a bond length of 1.556(1) Å,[21] whereas the octamethylcyclobutane has a bond length of 1.571 Å (by AM1).[22] In contrast, exceptionally long bond lengths (1.61–1.72 Å) have also been observed for *e.g.* phenyl substituted cyclobutanes and anthracene dimers.[23,24] From our analysis, however, such drastic elongations were not observed (Table 4). Nevertheless, in almost every case, one bond showed a significant elongation compared to the other bonds of the cyclobutane moiety. Cyclobutane **3c** shows a slight elongation of bond 1 (1.584(2) Å) compared to the other bonds (~1.55 Å). For cyclobutane **13**, bond 4 is elongated (1.579(2) Å). However, even though cyclobutane **11** showed a markedly higher oxidation potential, the same elongation of bond 4 was observed (1.585(1) Å). In this case, we attribute this to steric repulsion between the methyl and phenyl substituents at C1 and C4. Nevertheless, it may be possible, for cyclobutanes that relate to our investigated molecular structure, to correlate bond elongations for cyclobutanes with lower oxidation potentials to electronic rather than steric effects.[22] In fact, this can also be seen from the comparison of three cyclohexenone-based cyclobutanes (**9a–c**). All three substrates have a similar molecular structure, but a slightly altered electronic structure from 4-phenyl substitution. Therein, the most electron-rich cyclobutane **9c** shows the largest bond elongation compared to the least electron-rich cyclobutane **9b**.

Most noticeably, however, was the correlation of the dihedral angles and the redox potentials (Table 5). The lower the oxidation potential was, the more planar the cyclobutane-core seemed to be. This can further be correlated to the electron density of the products. For cyclobutane **13** (highest electron

Table 4 Bond lengths of the cyclobutane moiety[a]

Bond	**3c**	**13**	**11**	**9a**	**9b**	**9c_1**[b]	**9c_2**[b]	**9c_3**[b]	**9c_4**[b]
1	1.584	1.555	1.555	1.566	1.558	1.574	1.568	1.571	1.574
2	1.547	1.563	1.567	1.567	1.569	1.566	1.567	1.564	1.564
3	1.555	1.551	1.562	1.549	1.554	1.547	1.551	1.551	1.549
4	1.558	1.579	1.585	1.563	1.564	1.571	1.577	1.577	1.575

[a] From single crystal X-ray diffraction analysis. For numbering, see Fig. 1). Values were rounded with a margin of error of ±1–2 on the last digit (±4 for **9c**), precise data in Table S5 (ESI). [b] Four crystallographic independent structures were obtained per asymmetric unit.

Table 5 Dihedral angles of the cyclobutane moiety[a] and oxidation potentials[b]

Compound	3c	9a	9b	9c_1	9c_2	9c_3	9c_4	13	11
Dihedral angle [°]	5.4	5.8	12.8	5.7	5.3	4.5	5.3	4.9	22.2
E_{offset}(ox) [V]	1.43	1.46	>1.55	1.03	1.03	1.03	1.03	1.10	1.56

[a] From single crystal X-ray diffraction analysis. Mean values from the four individual cyclobutane angles are given. Precise data can be found in Table S6 (ESI). [b] From cyclic voltammetry (see Table 3).

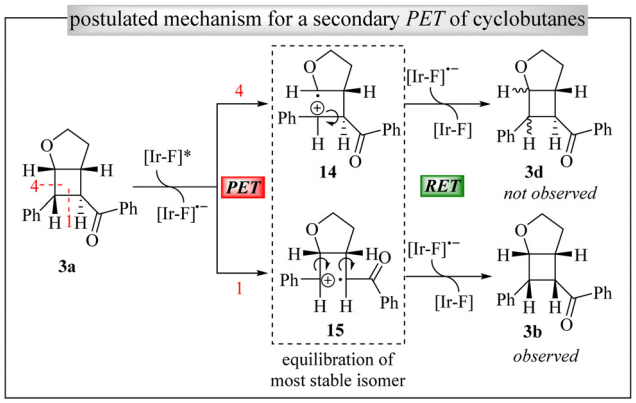

Scheme 2 Postulated mechanistic Scheme for a secondary PET reaction of cyclobutane photoproducts from the [Ir-F] photocatalyst.

density), the lowest oxidation potential and a small dihedral angle was observed (4.9°). In contrast, cyclobutane **11** (least electron-dense cyclobutane), has the largest dihedral angle and oxidation potential. This is confirmed by the series of cyclohexenone–cyclobutanes **9a–c**. A methoxy substitution resulted in reduced dihedral angles (~5.2°), whereas CF_3-substitution led to larger dihedral angles (12.8°). Further data, such as additional bond lengths and bond angles can be found in Tables S4–S6, ESI.†

Based on the data obtained from the reaction of chalcone (**1**) and 2,3-dihydrofuran (**2**), we postulate a mechanism that involves the oxidation of bond 1 by a reductive quenching of [Ir-F]* (Scheme 2). The so formed radical cation is anticipated to undergo σ-bond rotation to form the thermodynamically most stable conformation. After reversed electron-transfer (RET) by the $[Ir\text{-}F]^{\bullet-}$ radical anion, the cyclobutane is regenerated. For this process to occur, rotation processes as well as the RET has to occur in a short time-interval so that contact ion pair separation cannot take place. In contrast, oxidation of bond 4 would, after RET, lead to a new diastereomer **3d** with a loss in stereoinformation at C1 and C4. Since the formation of such a stereoisomer was not observed, the oxidation of bond 1 seems to be most likely.

In summary, we reported on the secondary photoreaction of the [2+2]-cycloaddition photoproducts of π^2(Acc)–π^2(Do) systems that we attributed to a PET process from the iridium photocatalyst. Whereas such processes have previously been observed in *e.g.* cycloreversion processes,[18] we were only able to observe a diastereoisomerization process instead of cycloreversion. This observation was only made after prolonged irradiation of the reaction mixture and highlights the complexity of photocatalytic reactions. While screening until complete conversion may be a practical method, it assumes that the photoproducts are stable. However, under highly energetic photocatalytic conditions, such assumptions must be verified by additional experiments under prolonged irradiation. Although we did so far not implement our findings in possible synthetic transformations for direct derivatisation of these cyclobutane products, such a secondary oxidation event could likely be utilised to insert nucleophiles directly into the photoproducts.

Conflicts of interest

There are no conflicts to declare.

Notes and references

1 T. Bach, *Synthesis*, 1998, 683–703.
2 S. Poplata, A. Troster, Y. Q. Zou and T. Bach, *Chem. Rev.*, 2016, **116**, 9748–9815.
3 M. J. James, J. L. Schwarz, F. Strieth-Kalthoff, B. Wibbeling and F. Glorius, *J. Am. Chem. Soc.*, 2018, **140**, 8624–8628.
4 D. Sarkar, N. Bera and S. Ghosh, *Eur. J. Org. Chem.*, 2020, 1310–1326.
5 Z. Lu and T. P. Yoon, *Angew. Chem., Int. Ed.*, 2012, **51**, 10329–10332.
6 N. E. S. Tay, D. Lehnherr and T. Rovis, *Chem. Rev.*, 2022, **122**, 2487–2649.
7 M. Neumann and K. Zeitler, *Chemistry*, 2013, **19**, 6950–6955.
8 J. Lefarth and A. G. Griesbeck, *J. Org. Chem.*, 2022, **87**, 8028–8033.
9 H. J. Timpe, K. P. Kronfeld, U. Lammel, J. P. Fouassier and D. J. Lougnot, *J. Photochem. Photobiol., A*, 1990, **52**, 111–122.
10 J. Luo and J. Zhang, *J. Org. Chem.*, 2016, **81**, 9131–9137.
11 N. A. Romero and D. A. Nicewicz, *Chem. Rev.*, 2016, **116**, 10075–10166.
12 M. S. Lowry, J. I. Goldsmith, J. D. Slinker, R. Rohl, R. A. Pascal, G. G. Malliaras and S. Bernhard, *Chem. Mater.*, 2005, **17**, 5712–5719.
13 N. A. Till, L. Tian, Z. Dong, G. D. Scholes and D. W. C. MacMillan, *J. Am. Chem. Soc.*, 2020, **142**, 15830–15841.
14 Since compound **3b** could only be isolated as a liquid and as a mixture with compound **3a**, further studies were performed with compound **3c** as a reference system instead of **3b**.
15 B. Kurpil, Y. Markushyna and A. Savateev, *ACS Catal.*, 2019, **9**, 1531–1538.
16 T. Lei, C. Zhou, M. Y. Huang, L. M. Zhao, B. Yang, C. Ye, H. Xiao, Q. Y. Meng, V. Ramamurthy, C. H. Tung and L. Z. Wu, *Angew. Chem., Int. Ed.*, 2017, **56**, 15407–15410.
17 K. Okada, K. Hisamitsu and T. Mukai, *Tetrahedron Lett.*, 1981, **22**, 1251–1254.
18 T. Hartman, M. Reisnerova, J. Chudoba, E. Svobodova, N. Archipowa, R. J. Kutta and R. Cibulka, *ChemPlusChem*, 2021, **86**, 373–386.
19 J. Lefarth, J. Neudörfl and A. G. Griesbeck, *Molbank*, 2021, **2021**, M1256.
20 A. D. McNaught and A. Wilkinson, *IUPAC. Compendium of Chemical Terminology (the "Gold Book")*, Blackwell Scientific Publications, Oxford, 2nd edn, 1997.
21 B. Vogelsanger, W. Caminati and A. Bauder, *Chem. Phys. Lett.*, 1987, **141**, 245–250.
22 S. Ōsawa, M. Sakai and E. Ōsawa, *J. Phys. Chem. A*, 1997, **101**, 1378–1383.
23 D. A. Dougherty, C. S. Choi, G. Kaupp, A. B. Buda, J. M. Rudziński and E. Ōsawa, *J. Chem. Soc., Perkin Trans. 2*, 1986, 1063–1070, DOI: 10.1039/p29860001063.
24 H. F. Bettinger, P. v R. Schleyer, H. F. Bettinger and H. F. Schaefer III, *Chem. Commun.*, 1998, 769–770, DOI: 10.1039/a800741a.

